

TECHNICAL NOTES

Open Access



Model-based myocardial T1 mapping with sparsity constraints using single-shot inversion-recovery radial FLASH cardiovascular magnetic resonance

Xiaoqing Wang^{1,2*}, Florian Kohler^{1,2}, Christina Unterberg-Buchwald^{1,2}, Joachim Lotz^{1,2}, Jens Frahm^{2,3} and Martin Uecker^{1,2}

Abstract

Background: This study develops a model-based myocardial T1 mapping technique with sparsity constraints which employs a single-shot inversion-recovery (IR) radial fast low angle shot (FLASH) cardiovascular magnetic resonance (CMR) acquisition. The method should offer high resolution, accuracy, precision and reproducibility.

Methods: The proposed reconstruction estimates myocardial parameter maps directly from undersampled k-space which is continuously measured by IR radial FLASH with a 4 s breathhold and retrospectively sorted based on a cardiac trigger signal. Joint sparsity constraints are imposed on the parameter maps to further improve T1 precision. Validations involved studies of an experimental phantom and 8 healthy adult subjects.

Results: In comparison to an IR spin-echo reference method, phantom experiments with T1 values ranging from 300 to 1500 ms revealed good accuracy and precision at simulated heart rates between 40 and 100 bpm. In vivo T1 maps achieved better precision and qualitatively better preservation of image features for the proposed method than a real-time CMR approach followed by pixelwise fitting. Apart from good inter-observer reproducibility (0.6% of the mean), in vivo results confirmed good intra-subject reproducibility (1.05% of the mean for intra-scan and 1.17, 1.51% of the means for the two inter-scans, respectively) of the proposed method.

Conclusion: Model-based reconstructions with sparsity constraints allow for single-shot myocardial T1 maps with high spatial resolution, accuracy, precision and reproducibility within a 4 s breathhold. Clinical trials are warranted.

Keywords: Model-based reconstruction, Myocardial T1 mapping, Sparsity constraint, Radial FLASH

Background

Quantitative myocardial T1 mapping finds increasing applications in clinical cardiovascular magnetic resonance (CMR) imaging. For example, native myocardial T1 mapping can be used to detect myocardial edema, while T1 maps after contrast agent are helpful for the detection of fibrosis and/or storage diseases [1, 2]. To date, developments have enabled fast cardiac T1 mapping in a clinically acceptable time, i.e., from 11 to 17 heartbeats

within one breathhold. Representative techniques include modified Look-Locker inversion recovery (MOLLI) [3], short modified Look-Locker inversion recovery (shMOLLI) [4], saturation recovery single-shot acquisition (SASHA) [5], and saturation pulse prepared heart rate independent inversion recovery (SAPPHIRE) [6]. Although MOLLI and variants are the most widely used techniques [2], they still face several challenges: (1) the occurrence of banding artifacts, in particular at high field strengths, which are due to balanced steady state free precession (bSSFP) off-resonance effects, (2) the underestimation of T1 values due to an imperfect physical modeling, and (3) a breathhold time of 11 to 17 heartbeats which may be challenging for patients.

* Correspondence: xiaoqing.wang@med.uni-goettingen.de

¹Department of Diagnostic and Interventional Radiology, University Medical Center Göttingen, Robert-Koch-Str. 40, 37075 Göttingen, Germany

²DZHK (German Centre for Cardiovascular Research), partner site Göttingen, Berlin, Germany

Full list of author information is available at the end of the article



Several ideas have been proposed to overcome these limitations. For example, replacing the bSSFP readout by a fast low angle shot (FLASH) acquisition completely avoids banding artifacts [7–11]. More complex physical models, which take care of the inversion efficiency or slice profile effects improve the accuracy of T1 estimation [8, 12]. More recently, non-Cartesian acquisition schemes (mainly radial) have been employed to enable fast myocardial T1 mapping [9–11]. Specifically, the combination of radial encoding with sliding window image reconstruction [10], compressed sensing [9] and real-time CMR [11] has enabled high-resolution myocardial T1 mapping within a single inversion-recovery (IR) relaxation process.

Model-based reconstructions [13–21] represent another strategy to accelerate quantitative parameter mapping in general. Such methods exploit inherent data redundancy by estimating parameter maps directly from an under-sampled k-space for a known signal model [14]. With respect to T1 mapping, it has been proposed to iteratively optimize model parameters by alternating between k-space and image-space [17] with applications to the brain and heart [22]. On the other hand, recent developments formulate T1 estimation as a nonlinear inverse problem [19–21, 23]. In this way, a priori information such as sparsity constraints can be easily incorporated into the reconstruction to increase performance and in particular improve T1 accuracy and precision.

In this work, we extend a previously developed method [20] for sparsity-constrained model-based T1 estimation to allow for cardiac applications. The data acquisition is based on a single-shot IR radial FLASH sequence and triggered to early diastole. The proposed method is validated for an experimental phantom at simulated heart rates and in vivo studies with 8 healthy subjects.

Methods

Data acquisition and model-based reconstruction

The single-shot IR scheme used here has been reported before [11]. For myocardial T1 mapping, data acquisition starts with a non-selective inversion pulse which is triggered to the early diastolic phase with use of a finger pulse signal. After inversion, the signal is continuously acquired for a period of 4 s using a radial FLASH readout with a golden-angle trajectory. To eliminate motion effects during systolic contraction and expansion, only data from the diastolic phase is retrospectively selected for T1 mapping.

The signal from multiple coils is given by

$$y_j(t) = \int M_{t_k}(\vec{r}) c_j(\vec{r}) e^{-i\vec{r}\vec{k}(t)} d\vec{r} \quad (1)$$

with c_j the j th coil sensitivity map, $\vec{k}(t)$ the chosen k-

space trajectory, $y_j(t)$ the acquired data and $M_{t_k}(\vec{r})$ the magnetization at time t_k after inversion

$$M_{t_k} = M_{ss} - (M_{ss} + M_0) \cdot e^{-t_k \cdot R_1^*} \quad (2)$$

where t_k is defined as center of the acquisition window in this study. M_{ss} , M_0 and R_1^* represent the steady-state signal, equilibrium signal and effective relaxation rate, respectively. After estimation of (M_{ss}, M_0, R_1^*) , T1 can be calculated by

$$T1 = \frac{M_0}{M_{ss} \cdot R_1^*} \quad (3)$$

In Eqs. (1) and (2), both the model parameters $(M_{ss}, M_0, R_1^*)^T$ and all coil sensitivity maps $(c_1, \dots, c_N)^T$ are unknowns, which are directly estimated from k-space using a sparsity constrained model-based reconstruction, i.e.,

$$\hat{x} = \operatorname{argmin} \|F(x) - y\|_2^2 + \alpha R(x_p) + \beta Q(x_c) \quad (4)$$

Here F is the nonlinear forward model mapping all unknowns to the measured data y :

$$F : x \mapsto \begin{pmatrix} P_1 \mathcal{F}\{c_1 \cdot M_{t_1}(M_{ss}, M_0, R_1^*)\} \\ \vdots \\ P_1 \mathcal{F}\{c_N \cdot M_{t_1}(M_{ss}, M_0, R_1^*)\} \\ P_2 \mathcal{F}\{c_1 \cdot M_{t_2}(M_{ss}, M_0, R_1^*)\} \\ \vdots \\ P_n \mathcal{F}\{c_N \cdot M_{t_n}(M_{ss}, M_0, R_1^*)\} \end{pmatrix} \quad (5)$$

with P the orthogonal projection onto the trajectory and \mathcal{F} the 2D Fourier transform. The unknowns $x_p = (M_{ss}, M_0, R_1^*)^T$ and $x_c = (c_1, \dots, c_N)^T$. $R(x_p)$ is a L1-Wavelet regularization which exploits joint sparsity in the parameter dimension following the ideas of compressed sensing, while $Q(x_c)$ is a Sobolev norm which is applied to the coil sensitivities to enforce their intrinsic smoothness. α and β are the corresponding regularization parameters. The nonlinear inverse problem in Eq. (4) is solved by the iteratively regularized Gauss-Newton method (IRGNM) [24] where the nonlinear problem is linearized in each Gauss-Newton step and solved by the fast iterative shrinkage-thresholding algorithm (FISTA) [25]. More details of the IRGNM-FISTA algorithm can be found in [20].

CMR

All CMR studies were conducted on a 3T system (Magnetom Skyra, Siemens Healthineers, Erlangen, Germany) with approval of the local ethics committee. Phantom measurements employed a 20-channel head/neck coil, while human heart studies used a combined thorax and spine coil with 26 channels. Eight subjects (three female, five male, age 27 ± 3 , range 23–32 years; heart rates

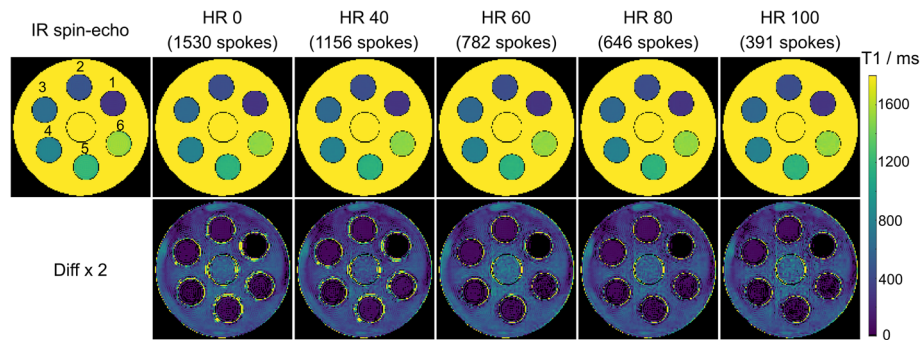


Fig. 1 (Top) Model-based T1 maps and (bottom) T1 difference maps ($\times 2$) for an experimental phantom and simulated heart rates (HR) in comparison to an inversion recovery (IR) spin-echo reference method

62 \pm 11 bpm, range 50–80 bpm) with no known illness were recruited. Written informed consent was obtained from all subjects prior to CMR. In vivo T1 measurements were performed within a single breathhold.

The proposed method was experimentally validated at simulated heart rates with a commercial reference phantom (Diagnostic Sonar LTD, Livingston, Scotland, UK) consisting of six compartments with defined T1 values surrounded by water. The gold standard T1 map for the phantom was estimated using an IR spin-echo method [26] with 9 IR scans (TI = 30, 530, 1030, 1530, 2030, 2530, 3030, 3530, 4030 ms), TR/TE = 4050/12 ms, FOV 192 \times 192 mm², matrix size 192 \times 192, and a total acquisition time of 2.4 h.

For IR radial FLASH, continuous data acquisition was performed with a tiny golden angle (18.71°) [27] after non-selective inversion. Because there is no intermediate image reconstruction, model-based reconstructions offer a flexible choice of temporal resolution, i.e., they allow a combination of an arbitrary (small) number of radial spokes for each k-space frame. However, as long as the T1 accuracy is not compromised, a certain degree of temporal discretization (data binning) is recommended to reduce the computational demand [19, 20]. In this study, 17 spokes formed one k-space and resulted in a temporal resolution of 45 ms. According to the subjects' heart rates, the resulting number of k-space frames were 48 \pm 9, range 33–57 for reconstructions in this study. Single-shot myocardial T1 maps of the

mid-ventricular slices were acquired at a nominal in-plane resolution of 1.0 \times 1.0 mm² and 8 mm slice thickness using a FOV 256 \times 256 mm² in combination with a resolution of 512 complex data points per radial spoke (two-fold oversampling). Other parameters were TR/TE = 2.67/1.67 ms, nominal flip angle 6°, bandwidth 850 Hz/pixel and total acquisition time 4 s.

To access reproducibility of the proposed method, the single-shot sequence was performed 3 times on each subject: The first two measurements were repeated one after the other, while the third one was done with a 5-min break, during which time the subject was taken out of the scanner. For comparisons, single-shot T1 maps were also estimated using the frame-based nonlinear inversion (NLINV) reconstruction with subsequent pixel-wise fitting as described in [11] without and with spatial filtering by a modified nonlocal means filter [28] from the same datasets. Further, a 5(3)3 MOLLI sequence provided by the vendor was applied for reference using a FOV of 360 \times 306.6 mm², in-plane resolution 1.41 \times 1.41 \times 8 mm³, TR/TE = 2.24/1.12 ms, nominal flip angle 35°, bandwidth 1085 Hz/pixel and total acquisition time 11 heart beats.

Implementation

All data was processed off-line. Multicoil raw data were first corrected for gradient delays [29] and then compressed to 10 virtual channels using a principal component analysis (PCA). A convolution-based gridding [30]

Table 1 T1 relaxation times (ms) for an experimental phantom and simulated heart rates

Tube	IR spin-echo	T2 [35]	HR 0	HR 40	HR 60	HR 80	HR 100
1	315 \pm 6	101 \pm 2	308 \pm 5	309 \pm 5	308 \pm 5	307 \pm 5	310 \pm 6
2	497 \pm 8	46 \pm 2	452 \pm 5	453 \pm 5	449 \pm 5	448 \pm 5	452 \pm 7
3	661 \pm 8	81 \pm 3	622 \pm 6	622 \pm 5	618 \pm 5	615 \pm 5	617 \pm 7
4	822 \pm 12	132 \pm 5	793 \pm 7	792 \pm 9	786 \pm 8	787 \pm 9	793 \pm 10
5	1191 \pm 13	138 \pm 4	1149 \pm 15	1140 \pm 15	1148 \pm 13	1153 \pm 15	1159 \pm 17
6	1508 \pm 15	166 \pm 5	1474 \pm 14	1462 \pm 16	1479 \pm 17	1474 \pm 17	1480 \pm 21

HR Heart rate, IR Inversion recovery

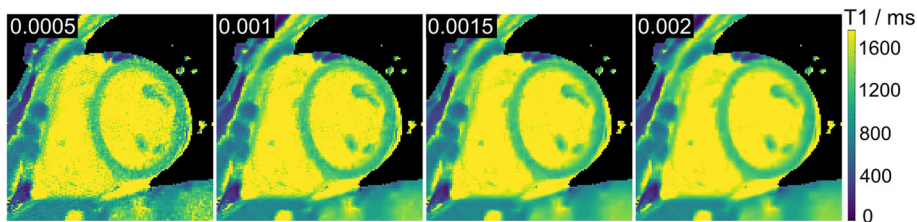


Fig. 2 Model-based myocardial native T1 maps as a function of the minimum regularization parameter α_{\min} . A value $\alpha_{\min} = 0.0015$ is used for all in vivo studies

without density compensation was used to interpolate the radial samples onto a Cartesian grid on which all successive iterations were performed. All the computations were done in Berkeley advanced reconstruction toolbox (BART) [31] on a 40-core 2.3 GHz Intel Xeon E5-2650 PC with a RAM size of 500 GB.

The parameter maps $(M_{ss}, M_0, R_1^*)^T$ were initialized with $(1.0, 1.0, 1.5)^T$ and all coil sensitivities zeros for all reconstructions. 10 Gauss-Newton steps were employed to ensure convergence. Similar to [20], regularization parameters α and β were initially set to 1 and subsequently reduced by a factor of 3 in each Gauss-Newton step. A minimum value of α was used to control the noise at higher Gauss-Newton steps. The chosen value of α_{\min} was defined by optimizing signal to noise ratio (SNR) without compromising quantitative accuracy or delineation of structural details. With the above settings, the whole computation took around 6 h using the CPUs. However, with a reduced number (e.g., 6) of virtual coils, computations could be run on a GPU, which took 10 to 20 min per dataset

Data analysis

Results in this work are reported as mean \pm standard deviation (SD). For the assessment of myocardial T1 values, the regions of interest (ROIs) in the inter-ventricular

septum were carefully selected to exclude the blood pool using arrShow [32] tool in MATLAB (MathWorks, Natick, Massachusetts, USA) and performed by two independent observers. Similar to [8, 33], the precision of T1 estimation was evaluated using coefficient of variation ($CV = SD_{ROI}/Mean_{ROI} \times 100\%$). The reproducibility error was calculated by $\sqrt{(\sum_{i=1}^{n_s} T1_{diff}^2(i))/n_s}$, where $T1_{diff}(i)$ is the T1 difference between different measurements, n_s is the number of subjects. Further, a repeated measures analysis of variance (ANOVA) with Bonferroni post hoc test was used for comparisons and a P value < 0.05 was considered significant.

In addition, edge sharpness was quantitatively measured for both the proposed model-based reconstruction and MOLLI. It was done by fitting each septal T1 line profile (starting from the blood pool to the middle of the myocardial septum) to a parameterized sigmoid function [34]: $s(x) = \frac{a}{1+e^{-k \cdot (b-x)}} + c$, where x is the length (unit: millimeter) along the line profile and $(a, b, c, k)^T$ are the fitting parameters: a determines the vertical range, b determines the center location, c defines the vertical offset and k quantifies the growth rate or sharpness of the edges (The higher $|k|$, the sharper the edges). The above nonlinear least square fitting was then performed in MATLAB (MathWorks) using the Levenberg-

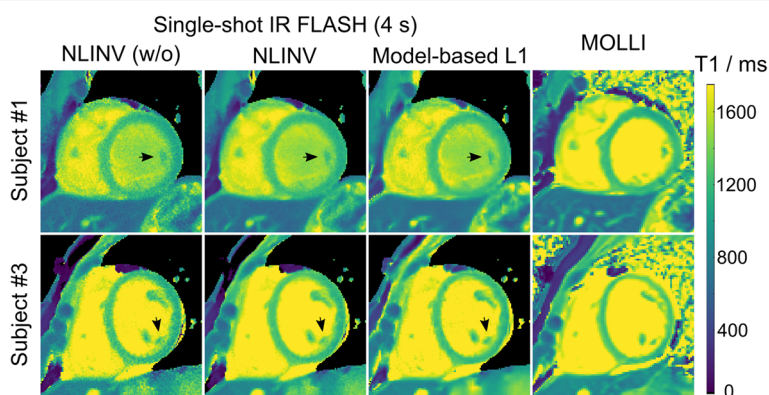


Fig. 3 Myocardial T1 maps obtained by single-shot IR radial fast low angle shot (FLASH) using (leftmost column) nonlinear inversion (NLINV) without spatial denoising and (middle left column) NLINV with spatial denoising and (middle right column) sparsity-constrained model-based reconstruction versus MOLLI. Black arrows indicate better preservation of image features for the proposed method

Table 2 Myocardial T1 values (ms) and CVs in left-ventricular septum of eight subjects using single-shot IR fast low angle shot (FLASH) with nonlinear inversion (NLINV) reconstruction without and with a spatial filter, the proposed model-based reconstruction and modified Look-Locker inversion recovery (MOLLI), respectively

Subject	Age/ years	HR/ bpm	NLINV(w/o)		NLINV		Model-based L1		MOLLI	
			T1 (ms)	CV	T1 (ms)	CV	T1 (ms)	CV	T1 (ms)	CV
1	32	55	1224 ± 55	4.5%	1232 ± 36	2.9%	1219 ± 35	2.9%	1215 ± 34	2.8%
2	24	55	1237 ± 63	5.1%	1249 ± 36	2.9%	1255 ± 36	2.9%	1212 ± 20	1.7%
3	23	50	1253 ± 61	4.9%	1268 ± 40	3.2%	1251 ± 41	3.3%	1242 ± 36	2.9%
4	30	58	1243 ± 82	6.6%	1248 ± 41	3.3%	1255 ± 38	3.0%	1226 ± 27	2.2%
5	25	60	1220 ± 73	6.0%	1224 ± 36	2.9%	1233 ± 36	2.9%	1189 ± 23	1.9%
6	27	55	1227 ± 73	5.9%	1242 ± 44	3.5%	1231 ± 39	3.2%	1195 ± 34	2.8%
7	25	80	1270 ± 82	6.5%	1268 ± 41	3.2%	1264 ± 42	3.3%	1245 ± 36	2.9%
8	27	80	1234 ± 88	6.1%	1224 ± 42	3.0%	1232 ± 45	3.2%	1210 ± 23	1.9%

Marquardt algorithm with a stopping criteria similar to [11].

Results

Figure 1 shows estimated T1 maps of an experimental phantom for different simulated heart rates between 40 and 100 bpm. The proposed technique is compared to a reference T1 map obtained by a conventional IR spin-echo method. Zero heart rate refers to a situation where no k-space data is deleted prior to model-based reconstruction. Visual inspection reveals good agreement for all heart rates and T1 values. These qualitative findings are confirmed by quantitative analyses summarized in Table 1. The maximum deviation between the proposed method and the reference is 10%. Noteworthy, good

precision is preserved at high heart rates for the proposed method. A long-axis T1 mapping was further performed (Additional file 1: Figure S1) to validate robustness of the proposed method. Both visual inspection and quantitative results (Additional file 3: Table S1) confirmed good T1 accuracy and precision in the long-axis view as well.

Figure 2 demonstrates the influence of the minimum regularization parameter α_{\min} used in sparsity – regularized model – based reconstructions. Low values of α_{\min} increase noise in the myocardial T1 maps, while high values lead to blurring. A value of $\alpha_{\min} = 0.0015$ was chosen to balance between noise reduction and preservation of image details. With these settings, Fig. 3 compares myocardial T1 maps of two representative subjects obtained by the proposed model-based reconstruction

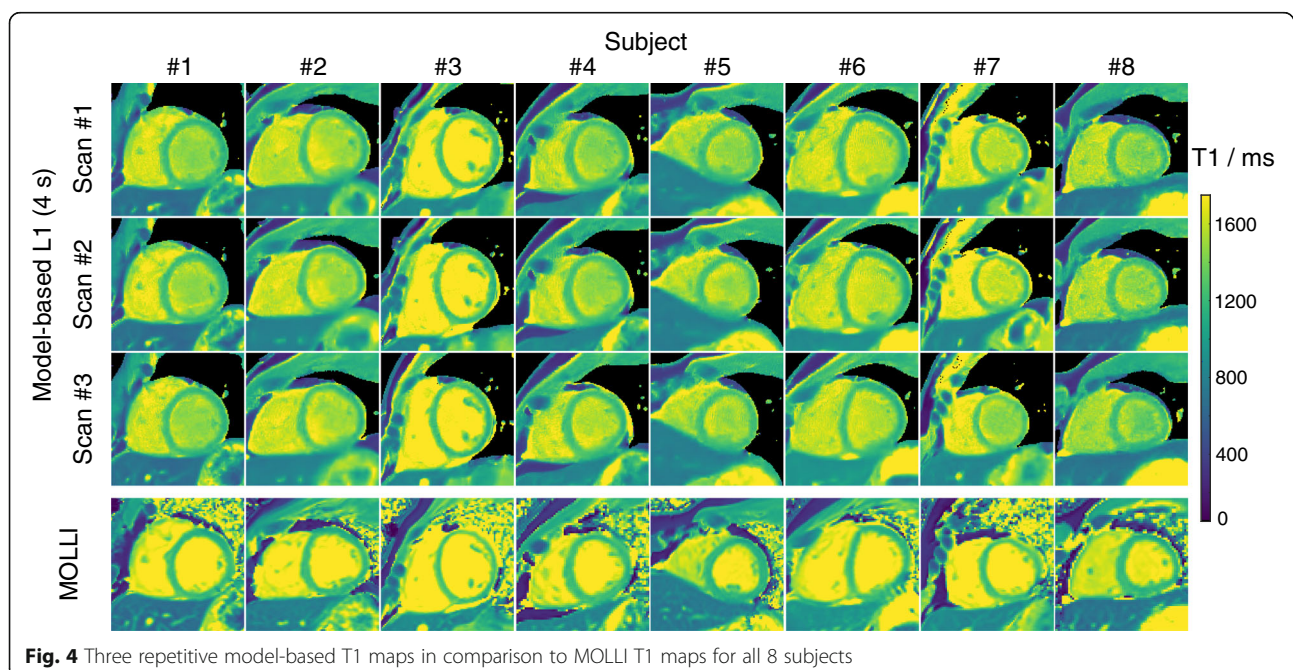
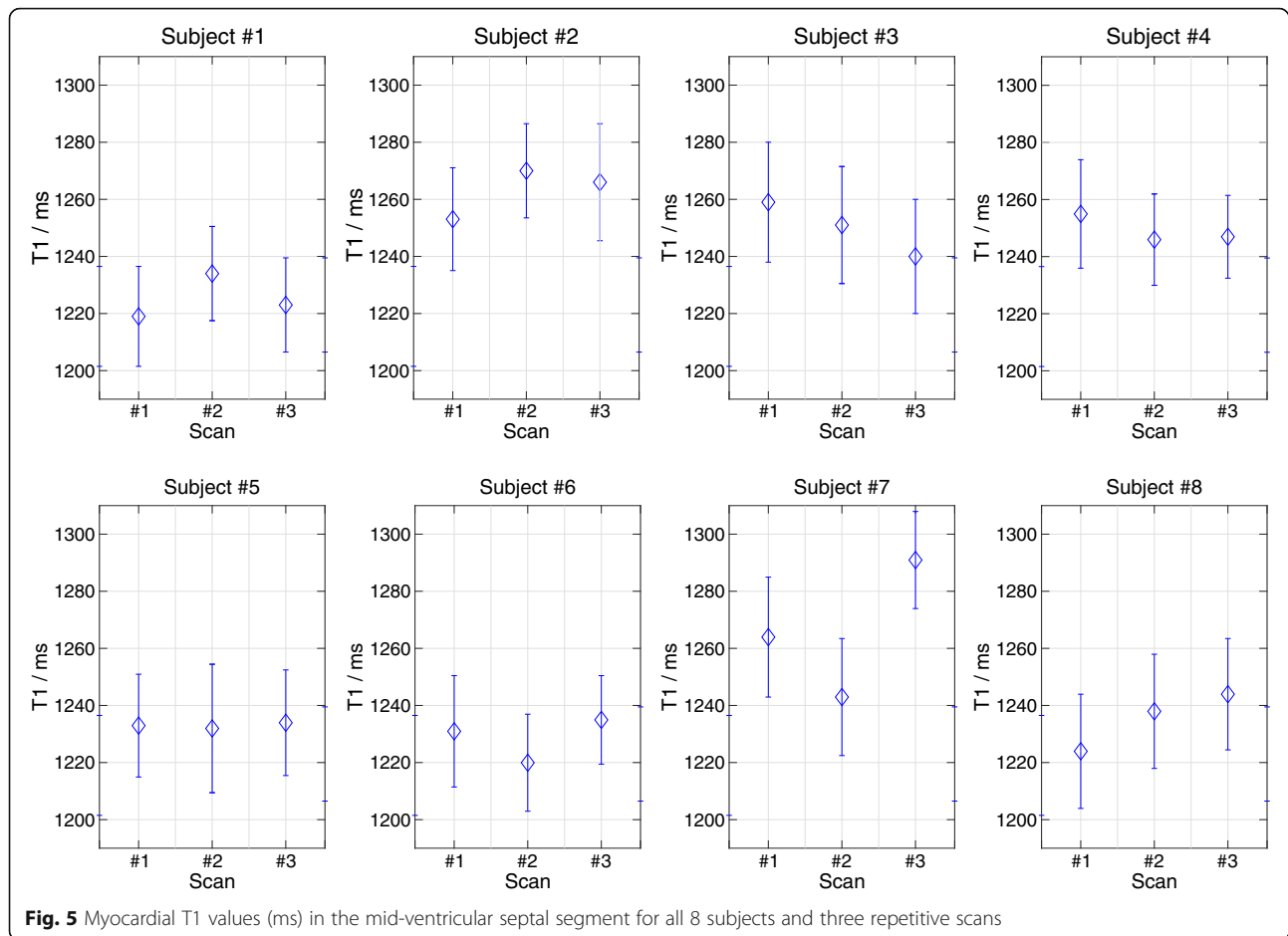


Fig. 4 Three repetitive model-based T1 maps in comparison to MOLLI T1 maps for all 8 subjects



versus a MOLLI technique and NLINV approaches without and with spatial filtering. In comparison to the NLINV approaches, model-based reconstructions generate T1 maps with visually less noise and better qualitative preservation of image features as indicated by black arrows. Table 2 shows quantitative T1 data for the left-ventricular septum of all subjects. The repeated measures ANOVA tests of the quantitative results revealed no significant difference among the quantitative mean myocardial T1 values by NLINV approaches and model-based reconstructions: NLINV (w/o) versus NLINV versus model-based: 1239 ± 16 versus 1244 ± 16 versus 1243 ± 15 ms ($p = 0.37$). However, the CV values are significantly different: NLINV (w/o) versus NLINV versus model-based: $5.7\% \pm 0.7\%$ versus $3.1\% \pm 0.2\%$ versus $3.1\% \pm 0.2\%$ ($p < 0.01$). A post hoc Bonferroni test confirmed that both the proposed model-based reconstruction and NLINV with the denoising filter have lower CV values, i.e., better T1 estimation precision than the NLINV method without spatial filtering ($p < 0.01$).

Figure 4 depicts a MOLLI T1 map and three repetitive T1 maps using the proposed method for all 8 subjects. The small visual difference among the repetitive scans

demonstrates good intra-subject reproducibility of the proposed method. These findings are quantitatively confirmed in Fig. 5 which presents mid ventricular septal T1 values for all subjects and all scans. The reproducibility errors for the proposed method are 14.3 ms (1.15% of the mean) for the intra-scan and 13.3 ms (1.07% of the mean), 18.8 ms (1.51% of the mean) for the two inter-scans respectively. Although slightly higher, the reproducibility errors are comparable to the corresponding values of MOLLI: 7.0 ms (0.6% of the mean), 11.7 ms (0.97% of the mean) and 13.9 ms (1.16% of the mean), respectively. Similarly, good inter-observer reproducibility was observed for both the proposed method and MOLLI, i.e., reproducibility error 7.5 ms (0.6% of the mean) and 6.4 ms (0.5% of the mean).

Figure 6 shows the sharpness measurements for all T1 maps by the proposed model-based reconstruction and MOLLI. Good correspondence was observed between the selected T1 line profiles and the fitted sigmoid curves for all datasets. The quantitative sharpness values $|k|$ presented below each T1 map revealed no significant difference between the proposed method and MOLLI (model-based versus MOLLI: 1.67 ± 0.68 versus $1.39 \pm 0.28 \text{ mm}^{-1}$, $p = 0.22$), indicating the proposed

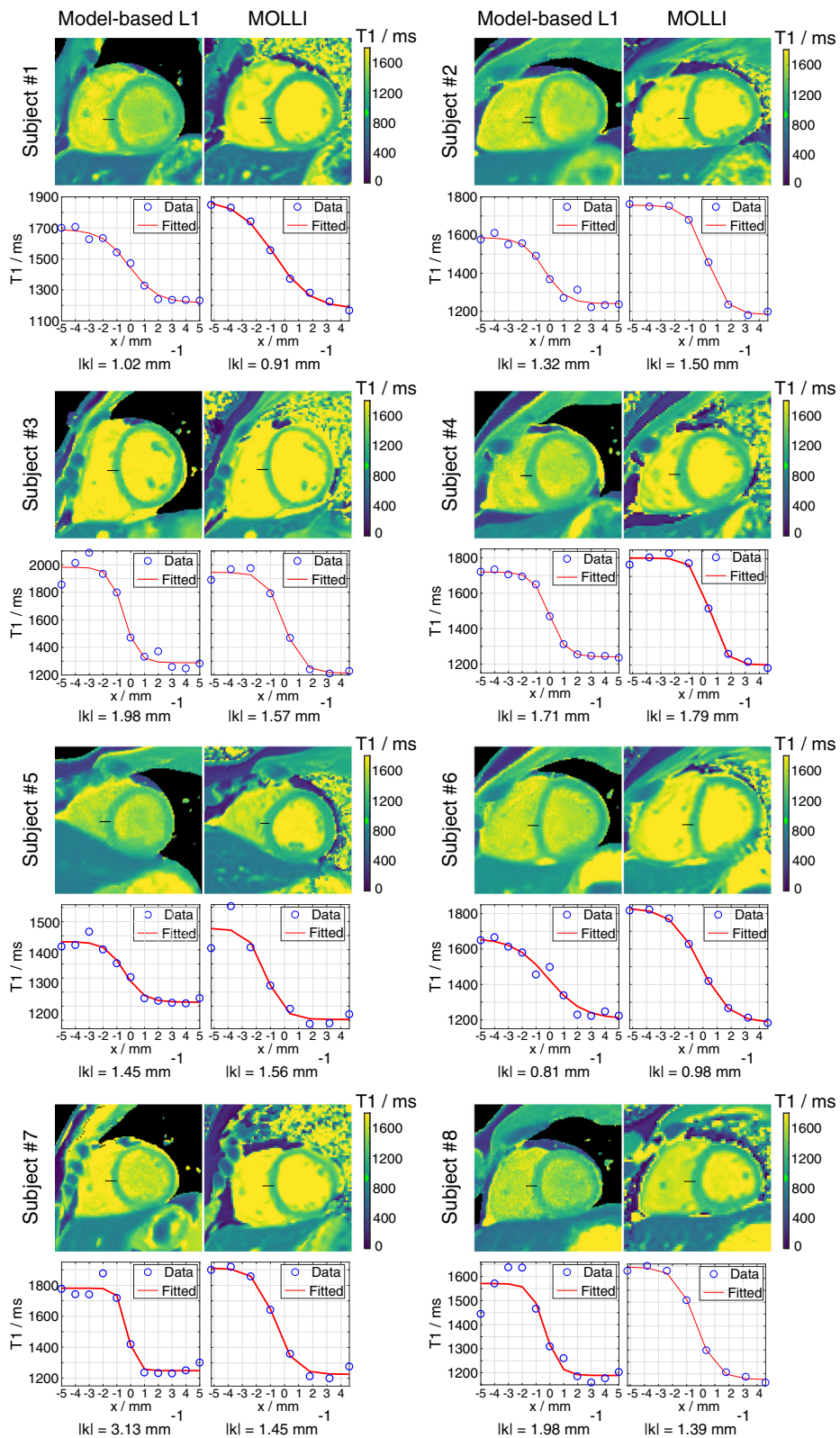


Fig. 6 Quantitative measurements of T1 edge sharpness for the proposed method and MOLLI for 8 subjects. For each subject, (top) T1 maps estimated by the two methods, (middle) selected T1 line profiles and the fitted sigmoid curves, (bottom) the quantitative sharpness values $|k|$. The selected line profiles are indicated by black lines on the T1 maps

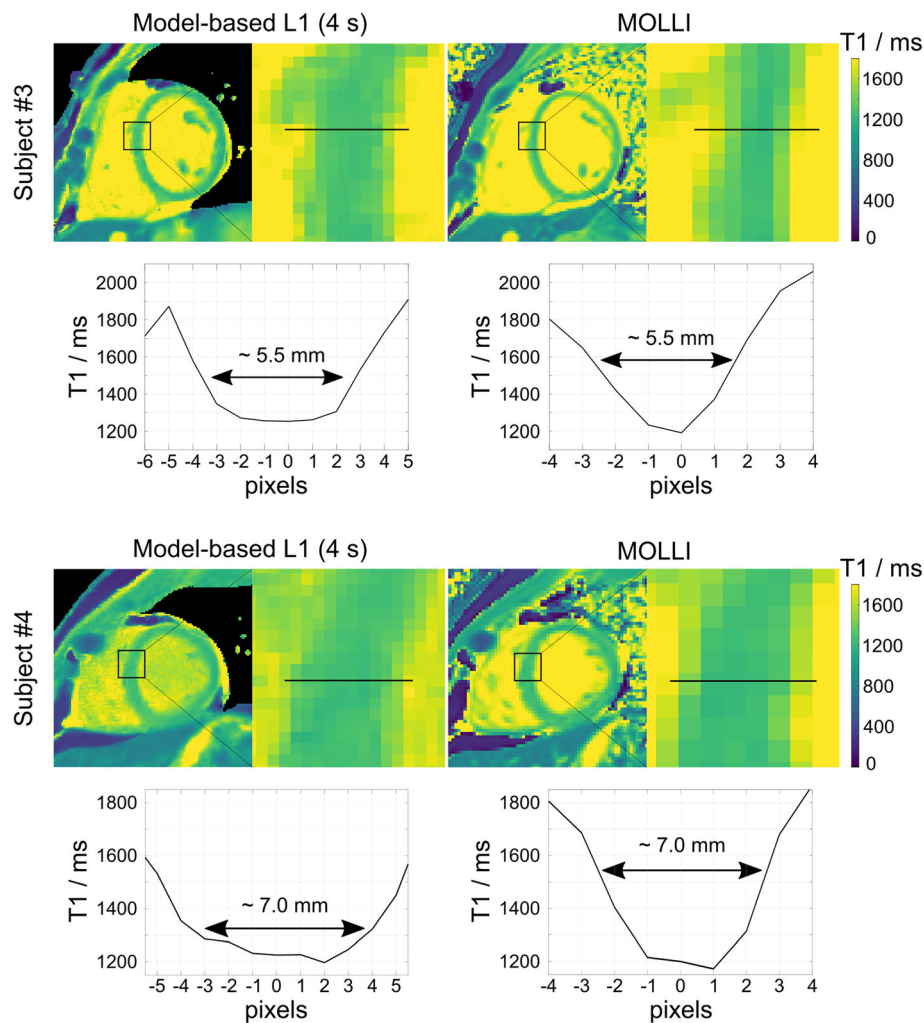


Fig. 7 (Top) Myocardial T1 maps and (bottom) selected T1 line profiles across the mid-ventricular septum by the proposed method and MOLLI

method produces T1 maps with comparable edge sharpness to MOLLI. Figure 7 further demonstrates estimated T1 maps and selected T1 line profiles across the myocardial septum by both methods for two representative subjects. More pixels are present across the septum by the model-based reconstructions, suggesting the proposed method should be helpful in reducing partial volume errors in myocardial T1 ROI measurements.

Apart from myocardial T1 maps, synthetic T1-weighted images can also be generated based on the signal Eq. (2) after model-based reconstructions. Figure 8a demonstrates four representative T1-weighted images starting from the beginning of inversion recovery to the time of dark blood, bright blood and steady state contrasts. The corresponding time points are also visible as dashed lines in the recovery curves in Fig. 8b. Both the dark blood and bright blood-weighted images clearly resolve contrasts between myocardium and blood pool (The whole image series with

a temporal resolution of 45 ms can be found in the Additional file 4: Video S1).

Discussion

This work presents a novel myocardial T1 mapping technique using a sparsity-constrained model-based reconstruction of a triggered single-shot IR radial FLASH acquisition. This method allows a flexible choice of temporal resolution as no intermediate image reconstruction is needed. Both studies on an experimental phantom and eight normal subjects demonstrate the proposed method could provide high-resolution myocardial T1 maps with good accuracy, precision, reproducibility and robustness within a measuring time of only 4 s. Plus, this method offers synthesized T1-weighted images with good contrast between myocardium and blood pool.

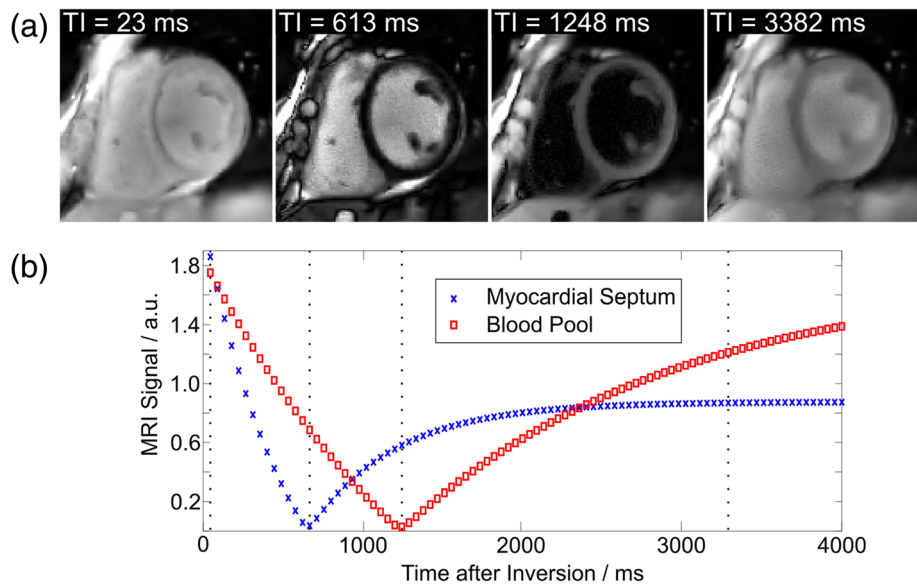


Fig. 8 a Synthesized T1-weighted images at four representative inversion times. **b** Signal evolutions of myocardial septum and blood pool (ROI averaged) during inversion recovery

The present method is very general and not limited to the single-shot sequence employed in this work. For example, it can also be combined with a MOLLI or SASHA sequence, as both share a similar IR signal model as used here. Moreover, also a Bloch-equation based signal model [8] can be integrated into the reconstruction framework. In that case, factors such as slice profiles and inversion efficiency may be taken into consideration for an even more accurate myocardial T1 mapping. On the other hand, a further improved efficiency may be achieved by combining the current model-based reconstruction with simultaneous multi-slice (SMS) techniques [36, 37]. Such strategies will allow for simultaneous single-shot myocardial T1 mapping within multiple sections.

This study mainly focuses on diastolic T1 mapping. However, when the heart rate gets higher, less diastolic data will be available within 4 s, making the proposed method more challenging, e.g., the resulting diastolic T1 maps will get slightly noisier (Additional file 2: Figure S2). One possible solution is to increase the regularization strength. On the other hand, systolic T1 mapping could be performed instead as more systolic data will be available in that case. Such investigations will be carried out on patients with higher heart rates in our future clinical studies.

The main limitations of the proposed method are the large memory demand and the long reconstruction time which are mainly caused by the need to hold the entire multi-coil IR data in memory during iterative

computation. Current implementations employ a PCA to compress the multi-coil data into several (here: 10) virtual channels to ameliorate the problem. However, the memory requirement is still high, which results in long computational time. Further optimization will include optimizing the algorithms, e.g., accelerating the linearized subproblem following the idea of T2 shuffling [38] as well as a more efficient GPU implementation.

Noteworthy, the estimated blood T1 values by the present sequence are not reliable as through-plane motion of blood flow would make the blood violate the assumed relaxation model. As a result, the present sequence may also be limited in the direct measurement of the myocardial extracellular volume (ECV). However, this might be a general problem for Look-Locker based approaches. The different blood T1 values between the proposed method and MOLLI can be attributed to the fact that the specific sequence used in the present work employed a continuous data acquisition scheme while MOLLI uses a triggered and prospective way for data acquisition.

The lack of motion estimation is another limitation for the proposed method. Although systolic data are retrospectively deleted prior to model-based reconstruction, residual nonrigid motion may still be present after sorting. This might be another reason why single-shot T1 maps by the proposed method appear slightly more blurred than motion-corrected MOLLI T1 maps provided by the vendor. Further investigation will either include a motion estimation into the model-based

reconstruction or perform a motion-resolved self-gated quantitative mapping strategy similar to XD-GRASP [39] or MR multitasking [40].

Conclusion

The proposed sparsity-constrained model-based reconstruction achieves single-shot myocardial T1 mapping within a 4 s breathhold. The method offers good accuracy, precision and reproducibility. More clinical trials are warranted.

Additional files

Additional file 1: Figure S1. Model-based long-axis T1 maps at heart rates (left top) 60 and (left bottom) 100 as well as (right) the corresponding T1 line profiles for the experimental phantom study. The quantitative T1 values are in the Additional file 3: Table S1. (PNG 100 kb)

Additional file 2: Figure S2. Myocardial T1 maps on a healthy subject by retrospectively rejecting an increasing amount of data prior to model-based reconstructions. The amount of data deleted corresponds to heart rates 50, 60, 80, 100 bpm, respectively. The ROI-analyzed septum T1 values are 1251 ± 41 ms, 1235 ± 43 ms, 1236 ± 49 ms and 1274 ± 53 ms for each reconstruction. (PNG 149 kb)

Additional file 3: Table S1. Long-axis T1 relaxation times (ms) for an experimental phantom and simulated heart rates 60 and 100. (DOCX 13 kb)

Additional file 4: Video S1. Synthesized T1-weighted image series at a temporal resolution of 45 ms. (AVI 30000 kb)

Abbreviations

ANOVA: Analysis of variance; BART: Berkeley advanced reconstruction toolbox; bpm: Beats per minute; bSSFP: Balanced steady State Free Precession; CMR: Cardiovascular magnetic resonance; CPU: Central processing unit; CV: Coefficient of variation; FISTA: Fast Iterative Shrinkage Thresholding Algorithm; FLASH: Fast low-angle shot; FOV: Field of view; GPU: Graphics processing unit; IR: Inversion-recovery; IRGNM: Iteratively regularized Gauss-Newton method; MOLLI: Modified Look-Locker inversion recovery; NLINV: Nonlinear inversion; PCA: Principle component analysis; SAPPHIRE: Saturation pulse prepared heart-rate-independent inversion recovery; SASHA: SATuration recovery Single-sHOT Acquisition; SD: Standard deviation; ShMOLLI: Shortened Modified Look-Locker inversion recovery; SNR: Signal-to-noise ratio; TE: Echo time; TR: Repetition time; XD-GRASP: EXtra Dimension-Golden angle Radial Sparse Parallel

Acknowledgements

We thank Dr. Sebastian Weingärtner for the insightful discussions during ISMRM 2018, Paris, France. We are also thankful for Yuxiao Luo for her help in quantitative ROI analyses.

Authors' contributions

XW developed the method, acquired, analyzed and interpreted the data, drafted and finalized the manuscript. FK, CU and JL were involved in the interpretation of the results and contributed to the manuscript. JF contributed to the design of the study and finalized the manuscript. MU designed the study, developed the method and contributed to the manuscript. All authors approved the manuscript before submission.

Funding

This work was supported by the DZHK (German Centre for Cardiovascular Research).

Availability of data and materials

In the spirit of reproducible research, the source code of the proposed method will be made available at: <https://github.com/mrirecon/myocardial-t1-mapping>.

Ethics approval and consent to participate

The study was approved by the local ethics committee of the University Medical Center Göttingen. Informed consent was obtained from all participants.

Consent for publication

Consent for publication was obtained from all participants in the study.

Competing interests

The authors declare that they have no competing interests.

Author details

¹Department of Diagnostic and Interventional Radiology, University Medical Center Göttingen, Robert-Koch-Str. 40, 37075 Göttingen, Germany. ²DZHK (German Centre for Cardiovascular Research), partner site Göttingen, Berlin, Germany. ³Biomedizinische NMR, Max-Planck-Institut für biophysikalische Chemie, Am Fassberg 11, 37077 Göttingen, Germany.

Received: 21 December 2018 Accepted: 31 July 2019

Published online: 19 September 2019

References

- Moon JC, Messroghli DR, Kellman P, Piechnik SK, Robson MD, Ugander M, Gatehouse PD, Arai AE, Friedrich MG, Neubauer S, et al. Myocardial T1 mapping and extracellular volume quantification: a society for cardiovascular magnetic resonance (SCMR) and CMR working group of the European Society of Cardiology consensus statement. *J Cardiovasc Magn Reson*. 2013;15:92.
- Kellman P, Hansen MS. T1-mapping in the heart: accuracy and precision. *J Cardiovasc Magn Reson*. 2014;16:2.
- Messroghli DR, Radjenovic A, Kozerke S, Higgins DM, Sivananthan MU, Ridgway JP. Modified look-locker inversion recovery (MOLLI) for high-resolution T1 mapping of the heart. *Magn Reson Med*. 2004;52:141–6.
- Piechnik SK, Ferreira VM, Dall'Armellina E, Cochlin LE, Greiser A, Neubauer S, Robson MD. Shortened Modified Look-Locker Inversion recovery (ShMOLLI) for clinical myocardial T1-mapping at 1.5 and 3 T within a 9 heartbeats breathhold. *J Cardiovasc Magn Reson*. 2010;12:1.
- Chow K, Flewitt JA, Green JD, Pagano JJ, Friedrich MG, Thompson RB. Saturation recovery single-shot acquisition (SASHA) for myocardial T1 mapping. *Magn Reson Med*. 2014;71:2082–95.
- Weingärtner S, Akçakaya M, Basha T, Kissinger KV, Goddu B, Berg S, Manning WJ, Nezafat R. Combined saturation/inversion recovery sequences for improved evaluation of scar and diffuse fibrosis in patients with arrhythmia or heart rate variability. *Magn Reson Med*. 2014;71:1024–34.
- Rodgers CT, Piechnik SK, DelaBarre LJ, Van de Moortele P-F, Snyder CJ, Neubauer S, Robson MD, Vaughan JT. Inversion recovery at 7 t in the human myocardium: measurement of T1, inversion efficiency and B1+. *Magn Reson Med*. 2013;70:1038–46.
- Shao J, Rapacchi S, Nguyen K-L, Hu P. Myocardial T1 mapping at 3.0 tesla using an inversion recovery spoiled gradient echo readout and Bloch equation simulation with slice profile correction (BLESSPC) T1 estimation algorithm. *J Magn Reson Imaging*. 2016;43:414–25.
- Marty B, Coppa B, Carlier P. Fast, precise, and accurate myocardial T1 mapping using a radial MOLLI sequence with FLASH readout. *Magn Reson Med*. 2018;79:1387–98.
- Gensler D, Mörchel P, Fidler F, Ritter O, Quick HH, Ladd ME, Bauer WR, Ertl G, Jakob PM, Nordbeck P. Myocardial T1: quantification by using an ECG-triggered radial single-shot inversion-recovery MR imaging sequence. *Radiology*. 2014;274:879–87.
- Wang X, Joseph AA, Kalentev O, Merboldt KD, Voit D, Roeloffs V, van Zalk M, Frahm J. High-resolution myocardial T1 mapping using single-shot inversion-recovery fast low-angle shot MRI with radial undersampling and iterative reconstruction. *Br J Radiol*. 2016;89:20160255.
- Marty B, Vignaud A, Greiser A, Robert B, de Sousa PL, Carlier PG. Bloch equations-based reconstruction of myocardial T1 maps from modified look-locker inversion recovery sequence. *PLoS One*. 2015;10:0126766.
- Block KT, Uecker M, Frahm J. Model-based iterative reconstruction for radial fast spin-Echo MRI. *IEEE Trans Med Imaging*. 2009;28:1759–69.
- Fessler JA. Model-based image reconstruction for MRI. *IEEE Signal Process Mag*. 2010;27:81–9.

15. Sumpf T, Uecker M, Boretius S, Frahm J. Model-based nonlinear inverse reconstruction for T2 mapping using highly undersampled spin-echo MRI. *J Magn Reson Imaging*. 2011;34:420–8.
16. Zhao B, Lam F, Liang ZP. Model-based MR parameter mapping with sparsity constraints: parameter estimation and performance bounds. *IEEE Trans Med Imaging*. 2014;33:1832–44.
17. Tran-Gia J, Wech T, Bley T, Köstler H. Model-based acceleration of Look-Locker T1 mapping. *PLoS One*. 2015;10:e0122611.
18. Ben-Eliezer N, Sodickson DK, Block KT. Rapid and accurate T2 mapping from multi-spin-echo data using Bloch-simulation-based reconstruction. *Magn Reson Med*. 2015;73:809–17.
19. Roeloffs V, Wang X, Sumpf T, Untenberger M, Voit D, Frahm J. Model-based reconstruction for T1 mapping using single-shot inversion recovery radial FLASH. *Int J Imaging Syst Technol*. 2016;26:254–63.
20. Wang X, Roeloffs V, Klosowski J, Tan Z, Voit D, Uecker M, Frahm J. Model-based T1 mapping with sparsity constraints using single-shot inversion-recovery radial FLASH. *Magn Reson Med*. 2018;79:730–40.
21. Wang X, Voit D, Roeloffs V, Uecker M, Frahm J. Fast interleaved multislice T1 mapping: model-based reconstruction of single-shot inversion-recovery radial FLASH. *Comput Math Methods Med*. 2018;2018:8. <https://doi.org/10.1155/2018/2560964>
22. Becker KM, Schulz-Menger J, Schaeffter T, Kolbitsch C. Simultaneous high-resolution cardiac T1 mapping and cine imaging using model-based iterative image reconstruction. *Magn Reson Med*. 2019;81:1080–91.
23. Maier O, Schoormans J, Schloegl M, Strijkers GJ, Lesch A, Benkert T, Block T, Coolen BF, Bredies K, Stollberg R. Rapid T1 quantification from high resolution 3D data with model-based reconstruction. *Magn Reson Med*. 2019;81:2072–89.
24. Bakushinsky AB, Kokurin MY. Iterative methods for approximate solution of inverse problems. Dordrecht: Springer; 2004.
25. Beck A, Teboulle M. A fast iterative shrinkage-thresholding algorithm for linear inverse problems. *SIAM J Imaging Sci*. 2009;2:183–202.
26. Barral JK, Gudmundson E, Stikov N, Etezadi-Amoli M, Stoica P, Nishimura DG. A robust methodology for in vivo T1 mapping. *Magn Reson Med*. 2010;64:1057–67.
27. Wundrak S, Paul J, Ulrici J, Hell E, Geibel MA, Bernhardt P, Rottbauer W, Rasche V. Golden ratio sparse MRI using tiny golden angles. *Magn Reson Med*. 2016;75:2372–8.
28. Klosowski J, Frahm J. Image denoising for real-time MRI. *Magn Reson Med*. 2017;77:1340–52.
29. Block KT, Uecker M. Simple method for adaptive gradient-delay compensation in radial MRI. In: Proceedings of the 19th annual meeting of ISMRM. Montreal; 2011. p. 2816.
30. Wajer F, Pruessmann KP. Major speedup of reconstruction for sensitivity encoding with arbitrary trajectories. In: Proceedings of the ISMRM 9th Annual Meeting. Glasgow; 2001. p. 767.
31. Uecker M, Ong F, Tamir J, Bahri D, Virtue P, Cheng J, Zhang T, Lustig M. Berkeley advanced reconstruction toolbox. In: Proceedings of the 23rd annual meeting of ISMRM. Toronto; 2015. p. 2486.
32. Sumpf T, Unterberger M. arrayshow: a guide to an open source matlab tool for complex MRI data analysis. In: Proceedings of the 21st annual meeting ISMRM. Salt Lake City; 2013. p. 2719.
33. Shao J, Liu D, Sung K, Nguyen K-L, Hu P. Accuracy, precision, and reproducibility of myocardial T1 mapping: a comparison of four T1 estimation algorithms for modified look-locker inversion recovery (MOLLI). *Magn Reson Med*. 2017;78:1746–56.
34. Ahmad R, Ding Y, Simonetti OP. Edge sharpness assessment by parametric modeling: application to magnetic resonance imaging. *Concepts Magn Reson Part A*. 2015;44:138–49.
35. Sumpf TJ, Petrovic A, Uecker M, Knoll F, Frahm J. Fast T2 mapping with improved accuracy using undersampled spin-echo MRI and model-based reconstructions with a generating function. *IEEE Trans Med Imaging*. 2014;33:2213–22.
36. Rosenzweig S, Holme HCM, Wilke RN, Voit D, Frahm J, Uecker M. Simultaneous multi-slice MRI using cartesian and radial FLASH and regularized nonlinear inversion: SMS-NLINV. *Magn Reson Med*. 2018;79:2057–66.
37. Weingärtner S, Moeller S, Schmitter S, Auerbach E, Kellman P, Shenoy C, Akçakaya M. Simultaneous multislice imaging for native myocardial T1 mapping: improved spatial coverage in a single breath-hold. *Magn Reson Med*. 2017;78:462–71.
38. Tamir JI, Uecker M, Chen W, Lai P, Alley MT, Vasanaawala SS, Lustig M. T2 shuffling: sharp, multicontrast, volumetric fast spin-echo imaging. *Magn Reson Med*. 2017;77:180–95.
39. Feng L, Axel L, Chandarana H, Block KT, Sodickson DK, Otazo R. XD-GRASP: Golden-angle radial MRI with reconstruction of extra motion-state dimensions using compressed sensing. *Magn Reson Med*. 2016;75:775–88.
40. Christodoulou AG, Shaw JL, Nguyen C, Yang Q, Xie Y, Wang N, Li D. Magnetic resonance multitasking for motion-resolved quantitative cardiovascular imaging. *Nat Biomed Eng*. 2018;2:215.

Publisher's Note

Springer Nature remains neutral with regard to jurisdictional claims in published maps and institutional affiliations.

Ready to submit your research? Choose BMC and benefit from:

- fast, convenient online submission
- thorough peer review by experienced researchers in your field
- rapid publication on acceptance
- support for research data, including large and complex data types
- gold Open Access which fosters wider collaboration and increased citations
- maximum visibility for your research: over 100M website views per year

At BMC, research is always in progress.

Learn more biomedcentral.com/submissions

